Turkish Journal of Electromechanics and Energy
ISSN: 2547-975X
Vol:9, No:3, Page 124-130 (2024)
https://www.scienceliterature.com

Indirect current controlled VSC-based RPFC for power management in a railway power supply system

A. P. Shayer[1,*], M. A. Mulla[1]

[1]*Department of Electrical Engineering, Sardar Vallabhbhai National Institute of Technology, Surat, India*

ARTICLE INFO

***Article Type*:**
Research paper

Article History:
Received: 10 November 2024
Revised: 13 December 2024
Accepted: 22 December 2024
Published: 31 December 2024

Editor of the Article:
M. E. Şahin

Keywords:
Current unbalance, Power flow control, Power quality, Railway electrification, Railway power system, RPFC, VSC

ABSTRACT

A traction substation manages the railway power flow control (RPFC) in electrical power system. Special transformers are used in a traction substation along with power electronics converters to achieve power balance and load reactive power compensation. This study introduces the use of a conventional three-phase substation transformer along with a three-leg, four-wire power converter to address the issues of power quality and current unbalance of a traction substation. The proposed topology's control algorithm is developed to draw balance power from the three-phase supply while supplying single-phase power to two traction sections. The converter regulates the flow of power such that the currents are drawn from all the phases of the transformer. The converter also provides support to the load-reactive power requirement. An indirect control of the voltage source converter (VSC) is adopted to reduce the computational burden of the control algorithm. The control algorithm is analytically studied. The system operation is analysed using a discrete simulation environment under different loading scenarios. The study is presented as a proof of concept.

Cite this article: A. P. Shayer, M. A. Mulla, " Indirect current controlled VSC-based RPFC for power management in a railway power supply system," *Turkish Journal of Electromechanics & Energy*, 9(3), pp.124-130, 2024.

1. INTRODUCTION

Historically, traction substation (TSS) sourced power from two phases of a three-phase high voltage (HV) grid and supplied a single-phase output to the traction load using a single-phase transformer. This system utilized a phase rotation technique to maintain an average power balance on the grid. However, as only two phases were used of the HV grid, absolute and instantaneous power balance was not achieved with this technique. To achieve a more balanced grid system, power needed to be drawn from all three phases of the HV grid. For this, a three-phase to single-phase or three-phase to two-phase conversion power supply was necessary. Converting a three-phase to a two-phase supply was more feasible considering the state of the art of transformer technology then. Various types of specialized transformers were introduced for this conversion. The two phases were then used to supply power to two sections of a traction line at a traction substation. The special transformer used were Scott, V-V, Le-Blanc, Woodbridge, YnVd, Yd, and multi-purpose balance transformer (MPBT) connections [1-6]. However, some of these connections inherently had primary sides unbalanced even when the secondary sides were loaded equally. Whereas those with balanced connections achieved primary side balance only when both secondary phases were equally loaded [7]. Achieving balanced loading on both phases of the traction transformer within a TSS proved difficult due to highly variable loading conditions. Later, power electronic converters were introduced to facilitate power transfer between secondary phases of the transformer. These schemes were termed railway power flow controller (RPFC) or co-phase (COP) railway system [8]. Additionally, they also tackled issues of reactive power compensation and harmonic mitigation. Both COP and RPFC configuration serves different loading conditions. While the co-phase system is used in high-speed rail networks wherein neutral sections are to be eliminated, the latter is used in more conventional rail networks, which have neutral sections.

Another advancement is in the area wherein flexible AC transmission (FACT) devices are used along with previously discussed systems to provide necessary compensation. Devices like APQC and SVC are connected at TSS as discussed in [2, 9-11]. In [12], the author has suggested connecting both 3ϕ APQC and SVC in parallel across both the secondaries of a VV transformer. [13] uses a UPQC-like configuration of both series hybrid converter SAC and shunt active filter SAF. Apart from active devices, researchers have also used passive devices to reduce the burden on converters by providing fixed compensation as discussed in [9, 14, 15].

Before the advent of power electronics, special transformers were used in railway power systems to address the unbalance issue. Later, power electronics were introduced in these existing systems to improve the power quality. This created an opportunity to replace the special transformer in the TSS with a conventional transformer, resulting in a reduction in capital cost and a better

*Corresponding author's e-mail: aliasgarshayer@gmail.com

material utilization factor (MUF) as compared to special transformers. The low MUF of special transformers like 81.6% for the Scott transformer, 84.5% for the Le Blanc transformer, and 82.6% for the Woodbridge transformer, led to the use of an impedance matching transformer, whose MUF is much higher at 91.95% [4]. The impedance matching (IM) transformer is a modified Y − Δ transformer. It is modified by adding extra windings on the Δ-side for impedance matching, which is then used to supply power to two phases on the secondary side. The number of turns of these additional windings is 0.366 times N, where N is the number of turns of each winding of the Δ - side connection of the transformer [4]. This results in a total of 24.4% increase in Δ - side winding as compared to a conventional Y − Δ transformer of the same rating. This configuration is widely used with an active, passive, or hybrid filter across the loads to address TSS power quality issues [2, 4, 11, 16-18]. However, the additional windings introduced increase the cost and size of the IM transformer and reduce the MUF. In the process of solving the limitations of the IM transformer, the purpose of using the conventional transformer is lost. However, in [19], a conventional Δ − Y transformer is used along with single-phase power electronics converters in a back-to-back configuration to control the power flow across the two secondary phases of the transformer. The MUF of this transformer is 92.8%, which is the highest among all transformers discussed [20]. As a result, the overall system efficiency would be the highest in TSS using the conventional Δ – Y transformer.

In [19], a co-phase system was proposed for a Δ − Y transformer-based traction substation. It used only two phases of the transformer secondary windings. In the proposed study, the same traction substation is used in a railway power flow controller configuration, utilizing all three secondary windings. In this Δ − Y transformer-based RPFC, two catenary sections of single-phase traction loads are connected to two different phases of the secondary transformer. A voltage source converter (VSC) is connected to three phases of the TSS transformer, to control the power flow between the three phases. The traction load uses the rail, which is earthed, as a return path. Thus, the return path of the load is connected to the transformer neutral point via earth, as it is also earthed. This loading configuration requires a four-wire operation, the fourth wire being the neutral wire. Such a configuration will require a three-phase VSC. A three-leg, four-wire split capacitor VSC is used for this purpose. The converter is coupled to the system using a coupling inductor. The control algorithm is developed using dual second-order generalized integrator-based positive sequence calculation (DSOGI-PSC).

The main contributions of this paper are as follows:

- A traction substation design, having a conventional Δ − Y transformer coupled to a three-leg four-wire voltage source converter. This topology can draw balanced power from the source even under unbalanced loading conditions.
- Maintaining an energy balance across the two DC link capacitors of the VSC, to counter the imbalance created due to unbalanced load conditions.
- A control algorithm to operate the converter such that balanced active power is drawn from the grid and load reactive compensation is performed by the VSC. This results in unity power factor operation and an improved voltage profile of the traction substation.

The paper is further organized as follows. The system design, principle of operation and control algorithm design are discussed in section two. A simulation study is discussed and results are analysed in section three. Section four is the conclusion of this work.

2. SYSTEM DESIGN OF THE PROPOSED RPFC

2.1. Power Circuit Design

Figure 1 shows an RPFC with a three-leg, four-wire split capacitor configuration. The three midpoints of each leg of the converter are connected to the three secondaries of the traction transformer using coupling inductors, and the neutral is connected to the midpoint of the DC link arrangement. The primary of the traction transformer is connected to the grid, and the two traction loads are connected to load-*a* and load-*b*, respectively. The line currents drawn from the grid are denoted as i_A, i_B, and i_C concerning the grid voltages v_A, $vB, and\ v_C$ which are the phase-to-neutral voltages. The secondary phase to neutral voltages are denoted as v_a, v_b, v_c and their respective phase currents are i_a, i_b, i_c. The converter currents are i_{Ca}, i_{Cb}, $and\ i_{Cc}$ and the two load currents are $i_{La}\ and\ i_{Lb}$. Three voltage sensors to measure v_a, v_b, v_c and five current sensors are used to measure i_a, i_b, i_c, i_{La}, $and\ i_{Lb}$.

2.2. Principle of Operation

The system operates on the principle that power flow on the secondary side of the transformer should be regulated such that a balanced supply of power is drawn on the primary side at the unity power factor. In the proposed system, when the converter is not operated, the system will draw currents from phase-*a* and phase-*b* only. As a result, highly unbalanced currents will be drawn from the grid supply. To draw balanced primary currents, secondary currents drawn should be balanced. To achieve this, the converter is used to manage the flow of power between the three secondary phases. The converter regulates the flow of power such that the currents are drawn from all three secondary phases and are balanced. Simultaneously, the converter also provides support to the load-reactive power requirement. This results in unity power factor operation. The converter is operated with secondary currents as reference, to reduce the computational burden of computing reference converter currents.

2.2. Control Algorithm Design

The task of the control algorithm is to control the VSC such that load requirements are fulfilled and balanced power is drawn from the source. To achieve this, a control algorithm is designed to perform the following tasks:

i) Calculate the ideal power to be drawn from the grid,

*ii) i*control the power flow in all the phases of VSC such that load reactive power is provided by the VSC and active power is drawn from the grid is balanced,

iii) Generate triggering signals for the VSC. A schematic diagram of the control algorithm is shown in Figure 2.

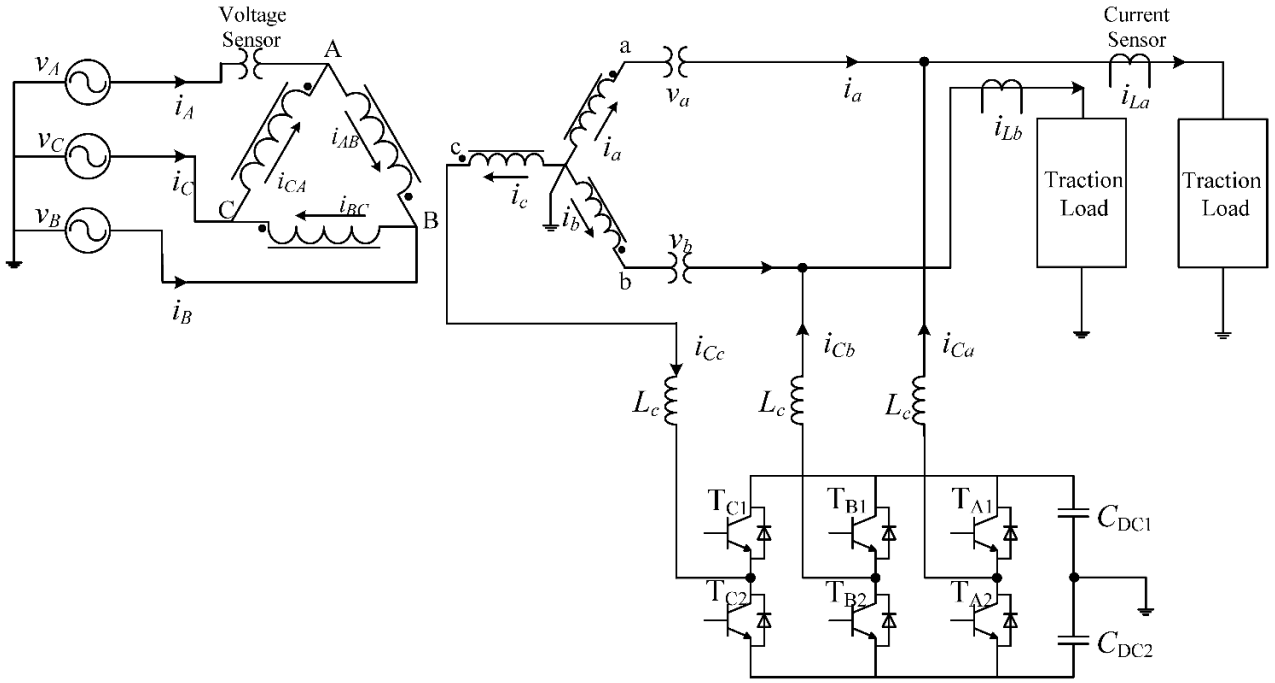

Fig. 1. Schematic diagram of an RPFC with a three-leg, four-wire split capacitor configuration.

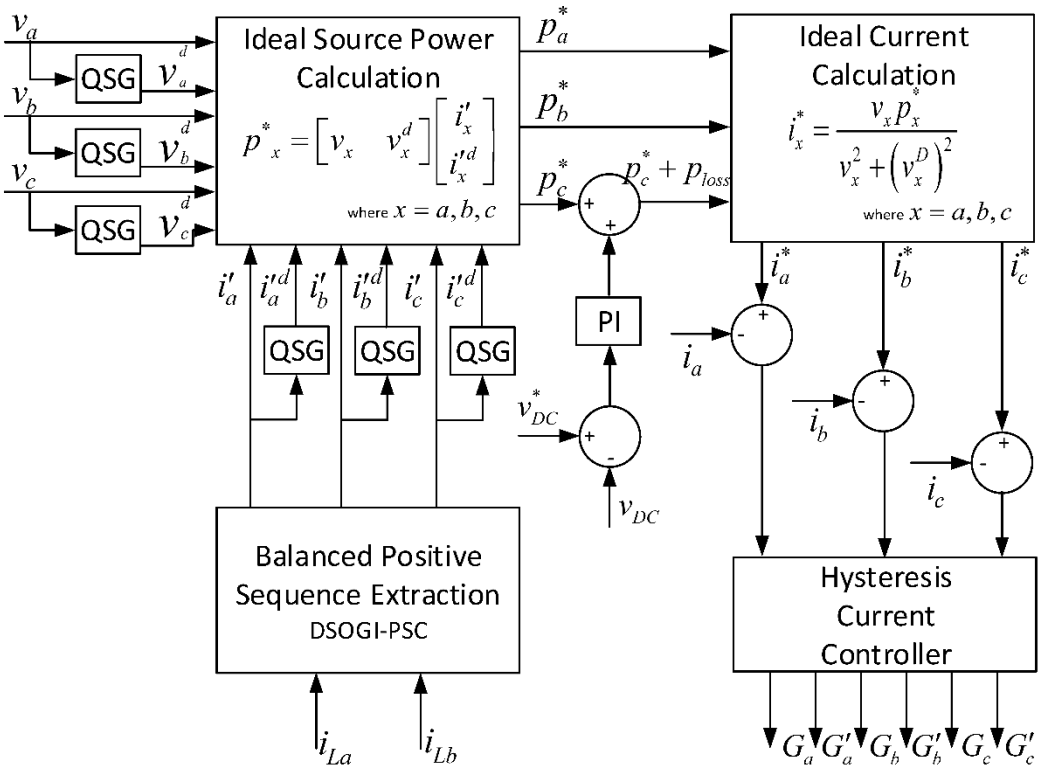

Fig. 2. Schematic diagram of the control algorithm for VSC control.

The first task is performed using DSOGI-PSC theory. It extracts the positive sequence component for a given set of 3-φ signals. This is used to find the positive sequence component of any distorted signal. The uniqueness of this control theory is that even for an unbalanced set of signals, the control algorithm gives a set of three balanced positive sequence signals. This feature is used in our application to determine the ideal positive sequence currents to be drawn from the grid even under highly unbalanced load conditions. The unbalanced condition in this load configuration is an extreme condition wherein one of the phases is heavily loaded, the second phase is lightly loaded, and the third phase is unloaded. The DSOGI-PSC has two functional components: *i*) the quadrature signal generator and *ii*) the positive sequence calculator, which are discussed further.

2.3.1. Quadrature signal generator (QSG)

A second-order generalized integrator (SOGI) is used for the quadrature signal generation [21]. Its characteristic transfer functions are given by Equation (1);

$$\frac{v'}{v}(s) = \frac{k\omega' s}{s^2 + k\omega' s + \omega'^2}; \quad \frac{qv'}{v}(s) = \frac{k\omega'}{s^2 + k\omega' s + \omega'^2} \tag{1}$$

Where ω' and k set resonance frequency and damping factor. $v, v',$ and qv' are the input, output and quadrature output signals respectively.

2.3.2. Positive sequence calculation (PSC)

Using the principle in [22], the instantaneous positive sequence component i^+_{abc} of a generic $3-\phi$ current vector $i_{abc} = [i_a i_b i_c]^T$ is given by;

$$i^+_{abc} = [i^+_a i^+_b i^+_c]^T = [T_+] i_{abc},$$
$$where\ [T_+] = \frac{1}{3}\begin{bmatrix} 1 & a^2 & a \\ a & 1 & a^2 \\ a^2 & a & 1 \end{bmatrix}, a = e^{-\frac{j2\pi}{3}} \tag{2}$$

Using the non-normalized Clarke transformation, the current vector can be translated from the abc to the $\alpha\beta$ reference frames as follows:

$$i_{\alpha\beta} = [i_\alpha i_\beta]^T = [T_{\alpha\beta}] i_{abc},$$
$$where [T_{\alpha\beta}] = \frac{2}{3}\begin{bmatrix} 1 & -\frac{1}{2} & -\frac{1}{2} \\ 0 & \frac{\sqrt{3}}{2} & -\frac{\sqrt{3}}{2} \end{bmatrix} \tag{3}$$

Therefore, the instantaneous positive-sequence current on the αβ reference frame can be calculated using Equation (2) and Equation (3) as,

$$i^+_{\alpha\beta} = [T_{\alpha\beta}] i^+_{abc} = [T_{\alpha\beta}][T_+] i_{abc}$$
$$= [T_{\alpha\beta}][T_+][T_{\alpha\beta}]^{-1} i_{\alpha\beta}$$
$$= \frac{1}{2}\begin{bmatrix} 1 & -q \\ q & 1 \end{bmatrix} i_{\alpha\beta}, q = e^{-\frac{j\pi}{2}} \tag{4}$$

where q is a phase-shift operator in the time domain which obtains the quadrature-phase signal (90-degree lag) of the original in-phase signal.

2.3.3. Positive sequence detector using DSOGI-PSC

The schematic of a positive sequence detector is shown in Figure 3. It uses a dual second-order generalized integrator (DSOGI) to provide input to the positive sequence calculation (PSC) in the $\alpha\beta$ frame of reference, which is then processed as per Equation (4), to obtain a balanced positive sequence component. The resultant signal is in $\alpha\beta$ reference frame. Hence, using inverse Clarke's transformation, the PSC is converted into i^+_{abc} in *the* abc frame of reference.

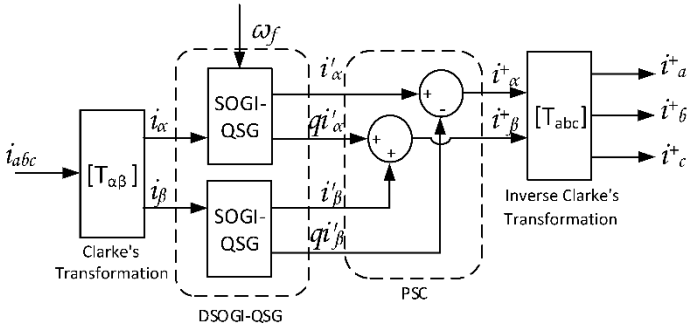

Fig.3. Block diagram of dual second-order generalized integrator-based positive sequence calculation (DSOGI-PSC).

2.3.4. Ideal power and reference current calculation

The control strategy for the three-leg four-wire (3L4W) VSC-based RPFC with DSOGI-PSC control theory is shown in Figure 2. Using the DSOGI-PSC block, the control theory calculates the balanced positive sequence currents. Then, second order generalized integrator (SOGI) based quadrature signal generator (QSG) is used to calculate the orthogonal components v^d_a, v^d_b, v^d_c of voltages and i'^d_a, i'^d_b, i'^d_c of currents. These signals, along with the in-phase signals v_a, v_b, v_c of voltages and i'_a, i'_b, i'_c of currents are then used to calculate the ideal power p^*_a, p^*_b, p^*_c which should be drawn from the source. These powers are calculated as,

$$p^*_x = [v_x \quad v^d_x]\begin{bmatrix} i'_x \\ i'^d_x \end{bmatrix}, \text{ where } x = a, b, c \tag{5}$$

These powers are then used to calculate the reference current $i^*_a,\ i^*_b,\ i^*_c$ to be drawn from the secondary traction transformer, so that balanced power is drawn from the grid. These currents are calculated as,

$$i^*_x = \frac{v_x p^*_x}{v^2_x + (v^d_x)^2}, \text{where } x = a, b, c \tag{6}$$

These currents are derived from the positive sequence components of the load current. Hence, it has only an active component of the load currents. The reactive component of load current is provided by the VSC. An indirect current control is adopted in this study; that is, the VSC is controlled using reference currents to be drawn from the source. As a result, load reactive power calculations are not required for reactive power compensation. Moreover, the power flow management between the three phases of the converter is also achieved by this indirect control without any power calculation for each phase of the converter. Thus, the second task of the control algorithm is achieved with reduced computational burden on the control algorithm.

The third task of the control algorithm is achieved by comparing the reference currents of Equation (6) with the actual secondary current i_a, i_b, i_c and the error is given to a hysteresis current controller which will generate triggering pulses $G_a,\ G'_a, Gb, Gb', Gc, G'_c$ for the switches $T_{A1},\ T_{A2},\ T_{B1},\ T_{B2},\ T_{C1},\ T_{C2}$ of VSC respectively.

3. RESULTS & DISCUSSION

A discrete simulation study was performed in MATLAB/ Simulink environment with a step-time of 10 μs, at a voltage level of 400 V AC from the grid. The transformation ratio of $\Delta - Y$ connected transformer is 1:1. The converter is connected at the point of common coupling via a coupling inductor. Phase-a is loaded with an inductive load of active power, p_{La} = 10 kW and reactive power q_{La} = 6.2 kVAr and phase-b is loaded with a light inductive load of active power, p_{Lb} = 2.5 kW and reactive power, q_{Lb} = 1.55 kVAr to emulate the highly variable traction load condition. The results are discussed for individual parameters. System Parameters are tabulated in Table 1. The system is tested for 500 ms, initially for 100 ms the system is in *non-balancing mode* and is uncompensated. At 100 ms the compensation is started and the system enters the *balancing mode*. At 250 ms, the loads on phase-a and phase-b are interchanged to study the dynamic response of the system.

Table 1. System parameters for simulation

Parameters	*Values*
Grid supply voltage, v_{LL}	400 V
Catenary supply voltage, v_L	230 V
Traction transformer $\Delta - Y$ in Dy1 configuration	400 / 400 V, 30 kVA
Coupling inductor, L	5 mH
DC link capacitor, C_{DC}	4700 µF
DC link voltage, V_{DC}	700 V
Inductive load-1	10 kW, 6.2 kVAr
Inductive load-2	2.5 kW, 1.55 kVAr

3.1. Load Parameters Analysis

Figure 4 shows the load voltages and currents for phase-a, v_{La}, i_{La} and phase-b, $v_{Lb}, and\ i_{Lb}$ respectively. The voltages are scaled to the ratio of 1:4 for the convenience of observation. The load angle is kept constant throughout the study at 0.8 lagging power factor. It is observed that the load voltages remain undistorted.

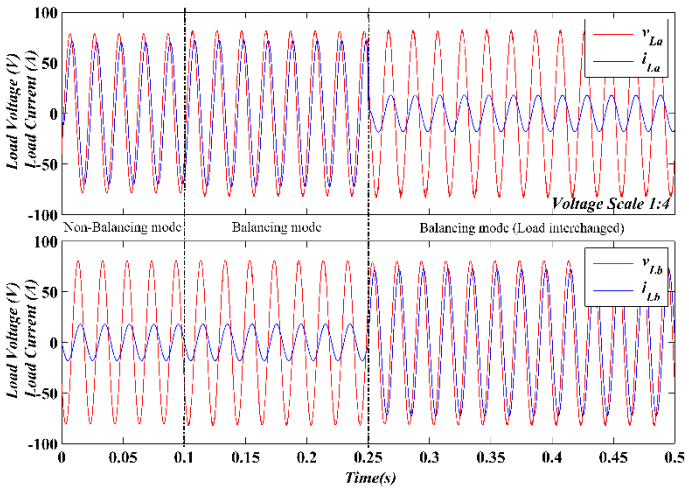

Fig. 4. Load voltage and current of phase-a and phase-b.

3.2. Active and Reactive Power Analysis

Figure 5 shows the active and reactive powers of source, p_s, q_s; of load-a, p_{La}, q_{La}; and of load-b, p_{Lb}, q_{Lb}. It is observed that under the balancing mode of operation, the active power drawn from the source is equal to the sum of load powers. The plot of reactive power shows that power drawn reduces to zero under the balancing mode of operation, that is, the reactive compensation is successfully carried out by the control algorithm.

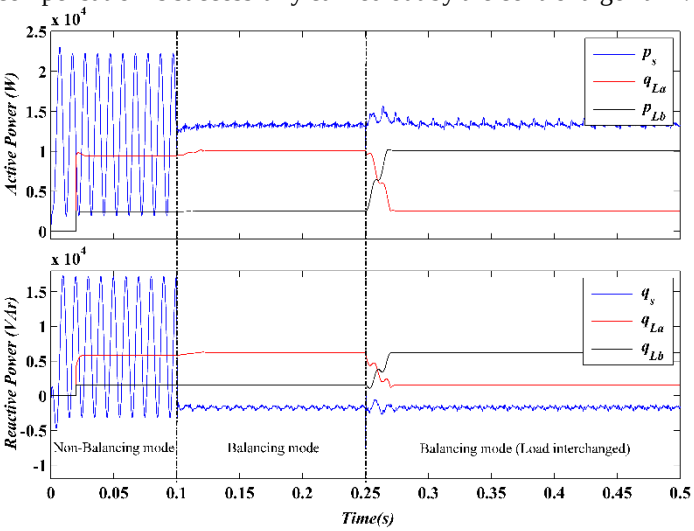

Fig. 5. Active power and reactive power of source, load-a, and load-b.

3.3. DC Link Voltage Analysis

In Figure 6, the first plot shows the DC link voltage of the VSC, v_{DC}. The DC link is maintained to the reference value throughout the system operation. The individual capacitor voltages, v_{DC1} and v_{DC2} are shown in the second plot. It is observed that the average voltage across capacitors C_{DC1} and C_{DC2} is equal. This shows that an average energy balance is maintained between the two capacitors even under unbalanced power flow through each leg of VSC.

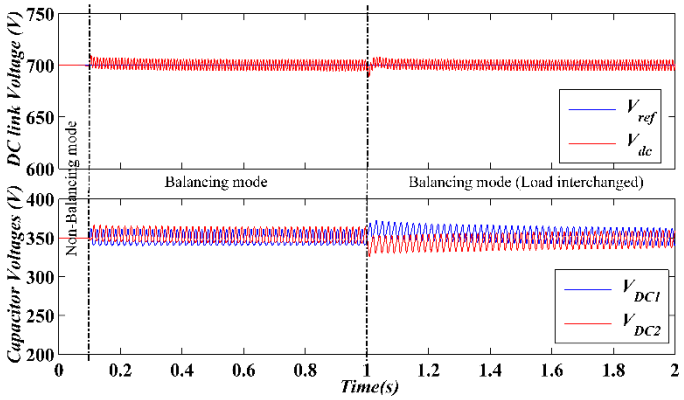

Fig. 6. DC link voltage and individual capacitor voltages of VSC.

3.4. Sequence Component Analysis

Figure 7 shows positive, negative and zero sequence components of source current, I_s^+, I_s^-, I_s^0; of load current, I_L^+, I_L^-, I_L^0; and of converter current, I_C^+, I_C^-, I_C^0. From the first plot it is observed that under the balancing mode of operation, the

positive sequence component of converter current I_C^+ is half that of load current I_L^+. This shows that only half the load active power is processed by the converter to achieve power balance. In the second plot, it is observed that the whole of load negative sequence I_L^- is compensated by the converter, and source I_S^- is zero. In the third plot, the zero sequence components are shown. The load currents' zero sequence component contributes to the DC link energy unbalance across the two split capacitors. It is observed here that the converter compensates the load currents' zero sequence components I_L^0. Thus, achieving an energy balance across the two DC link capacitors, as observed in the second plot of Figure 6.

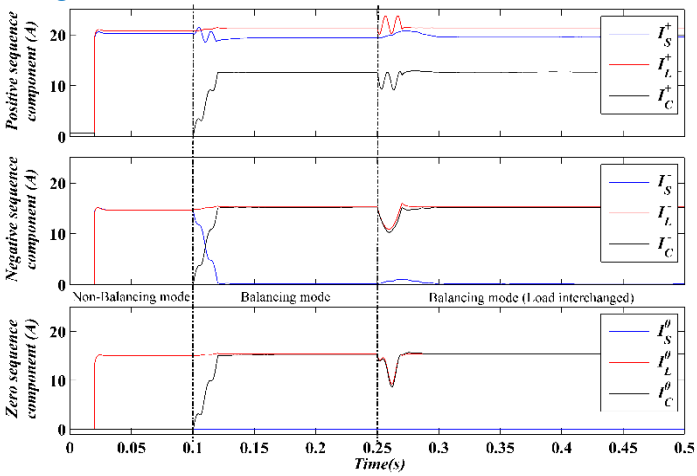

Fig.7. Positive, negative and zero sequence components of source currents, load currents, and converter currents.

3.5. Analysis of Secondary Parameters of Traction Transformer

Figure 8 shows the secondary $3-\phi$ voltages v_a, v_b, v_c in the first plot and currents i_a, i_b, i_c in the second plot, of the traction transformer. The voltage profile improves under the balancing mode of operation as compared to the non-balancing mode of operation. This is due to the reactive power compensation of the load, resulting in an improvement in the voltage profile. From the current plot it is observed that under the non-balancing mode of operation, the currents are highly unbalanced with phase-c current as zero. The currents become balanced under the balancing mode of operation. The balance is maintained under a steady state and dynamic load change condition.

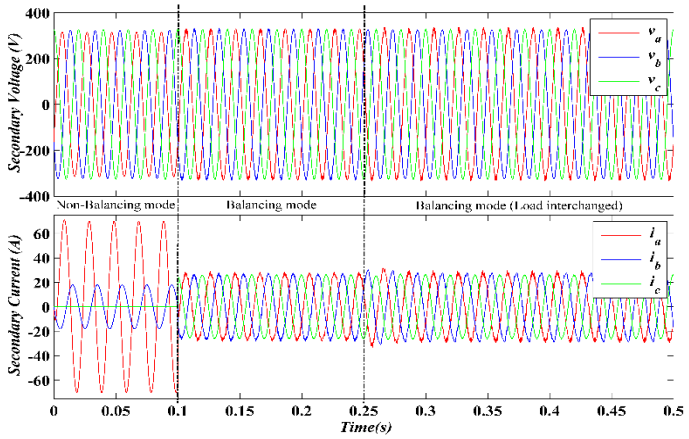

Fig. 8. Transformer secondary 3-ϕ voltages and currents.

3.6. Analysis of Grid Parameters

Figure 9 shows the $3-\phi$ currents $i_A, i_B, and\ i_C$ of the grid in the first plot. It is observed that the currents are balanced throughout the balancing mode of operation. The unbalance factors of grid voltage and current are shown in the second plot of Figure 9. It is observed that in non-balancing mode the current unbalance factor (CUF) is above 70%, whereas under balancing mode the CUF is within 4%. This factor is well within the limits of NEMA MG 1 2016 [23]. Based on the voltage unbalance factor (VUF) as observed in the second plot of Figure 9, which is zero throughout the system operation, it is concluded that the voltage remains balanced.

Thus, analysis of the results shows that the control algorithm can perform its tasks successfully. The system operates at unity power factor with complete load reactive power compensated. Balanced power is drawn from the grid supply with CUF well within the prescribed limits.

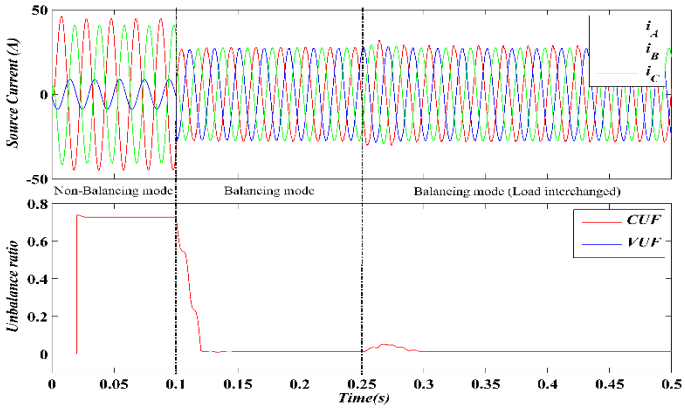

Fig. 9. Grid currents and their current unbalance factor (CUF) along with voltage unbalance factor (VUF).

4. CONCLUSION

In this study, power flow in a traction substation is managed using a three-leg four-wire VSC. A control algorithm is developed for this topology which aims to draw balanced power from the grid. A discrete closed-loop simulation is performed, and analysis of the results shows that the current drawn from the grid is balanced and at unity power factor. The negative and zero sequence components of load currents are compensated by the VSC, and the positive sequence component is only drawn from the source. The flow of active power from the source is controlled between the three phases of the converter and the two loads to fulfil the system requirements of a balanced grid and unity power factor operation. The voltage profile is improved due to reactive power compensation. Energy balance is maintained in the two capacitors of the DC link of VSC. The results validate the satisfactory operation of the control algorithm in steady-state and dynamic load variation conditions.

References

[1] A. Beirami, H. Feshki Farahani, "Adaptive hysteresis band current control-based power conditioner to improve the power quality of V/V railway supply system," *International Journal of Circuit Theory and Applications*, 46(8), pp. 1551-1564, 2018.

[2] B. Xie, Z. Zhang, S. Hu, Y. Li, L. Luo, S. Sun, "Yn/vd connected balance transformer-based electrical railway negative

sequence current compensation system with passive control scheme," *IET Power Electronics*, 9(10), pp. 2044-2051, 2016.
[3] S. M. M. Gazafrudi, A. T. Langerudy, E. F. Fuchs, K. Al-Haddad, "Power quality issues in railway electrification: A comprehensive perspective," *IEEE Transactions on Industrial Electronics*, 62(5), pp. 3081-3090, 2015.
[4] Z. Zhang, B. Wu, J. Kang, L. Luo, "A multi-purpose balanced transformer for railway traction applications," *IEEE Transactions on Power Delivery*, 24(2), pp. 711-718, 2009.
[5] W.-S. Chu, J.-C. Gu, "A new hybrid SVC scheme with Scott transformer for balance improvement," *Proceedings of the 2006 IEEE/ASME Joint Rail Conference*, Atlanta, GA, USA, 2006, pp. 217-224.
[6] B.-K. Chen, B.-S. Guo, "Three phase models of specially connected transformers," *IEEE Transactions on Power Delivery*, 11(1), pp. 323-330, 1996.
[7] G. Firat, G. Yang, H. A. H. Al-Ali, "A comparative study of different transformer connections for railway power supply-mitigation of voltage unbalance," *10th International Conference on Advances in Power System Control, Operation Management* (APSCOM 2015), Hong Kong, 2015, pp. 1-6.
[8] H. Hu, Y. Liu, Y. Li, Z. He, S. Gao, X. Zhu, H. Tao, "Traction power systems for electrified railways: evolution, state of the art, and future trends," *Railway Engineering Science*, 32(1), pp. 1-19, 2024.
[9] M. Habibolahzadeh, H. M. Roudsari, A. Jalilian, "Hybrid SVC-HPQC scheme with partial compensation technique in co-phase electric railway system," *27th Iranian Conference on Electrical Engineering (ICEE)*, Yazd, Iran, 2019, pp. 679-684.
[10] S. Hu, Y. Li, B. Xie, M. Chen, Z. Zhang, L. Luo, Y. Cao, A. Kubis, C. Rehtanz, "A Yd multifunction balance transformer-based power quality control system for single-phase power supply system," *IEEE Trans. on Ind. Appl.*, 52(2), pp. 1270-1279, 2016.
[11] S. Hu, Z. Zhang, Y. Chen, G. Zhou, Y. Li, L. Luo, Y. Cao, B. Xie, X. Chen, B.Wu, et al., "A new integrated hybrid power quality control system for electrical railway," *IEEE Transactions on Industrial Electronics*, 62(10), pp. 6222-6232, 2015.
[12] A. T. Langerudy, et al., "Hybrid railway power quality conditioner for high capacity traction substation with auto-tuned dc-link controller," *IET Electrical Systems in Transportation*, 6(3), pp. 207-214, 2016.
[13] B. Xie, Y. Li, Z. Zhang, S. Hu, Z. Zhang, L. Luo, Y. Cao, F. Zhou, R. Luo, L. Long, "A compensation system for cophase high-speed electric railways by reactive power generation of SHC & SAC," *IEEE Trans. on Industry. Elec.*, 65(4), pp. 2956-66, 2018.
[14] M. Habibolahzadeh, H. M. Roudsari, A. Jalilian, S. Jamali, "Improved railway static power conditioner using c-type filter in Scott co-phase traction power supply system," *10th International Power Electronics, Drive Systems and Technologies Conference (PEDSTC)*, Shiraz, Iran, 2019, pp. 355-360.
[15] S. Hu, Z. Zhang, Y. Li, L. Luo, P. Luo, Y. Cao, Y. Chen, G. Zhou, B. Wu, C. Rehtanz, "A new railway power flow control system coupled with asymmetric double LC branches, *IEEE Transactions on Power Electronics*, 30(10), pp. 5484-5498, 2015.
[16] Z. Zhang, B. Xie, S. Hu, Y. Li, L. Luo, C. Rehtanz, O. Krause, "Reactive power compensation and negative-sequence current suppression system for electrical railways with YNvd-connected balance transformer-part I: Theoretical analysis," *IEEE Transactions on Power Electronics*, 33(1), pp. 272-282, 2018.
[17] B. Xie, Z. Zhang, Y. Li, S. Hu, L. Luo, C. Rehtanz, O. Krause, "Reactive power compensation and negative-sequence current suppression system for electrical railways with YNvd-connected balance transformer-Part II: Implementation and verification," *IEEE Transactions on Power Electronics*, 32(12), pp. 9031-9042, 2017.
[18] Z. Sun, X. Jiang, D. Zhu, G. Zhang, "A novel active power quality compensator topology for electrified railway," *IEEE Transactions on Power Electronics*, 19(4), pp. 1036-1042, 2004.
[19] A. P. Shayer, M. A. Mulla, "Δ-Y transformer-based railway co-phase power system," *Arabian Journal for Science and Engineering*, 49(12), pp. 16533-16548, 2024.
[20] L. Guangye, Y. Yihan, "Three-phase-to-four-phase transformer for four-phase power-transmission systems," *IEEE Transactions on Power Delivery*, 17(4), pp. 1018-1022, 2002.
[21] X. Yuan, W. Merk, H. Stemmler, J. Allmeling, "Stationary-frame generalized integrators for current control of active power filters with zero steady-state error for current harmonics of concern under unbalanced and distorted operating conditions," *IEEE Transactions on Industry Applications*, 38(2), pp. 523-532, 2002.
[22] W. V. Lyon, "Applications of the method of symmetrical components," *McGraw-Hill Book Company*, 1937.
[23] H. Arghavani, M. Peyravi, "Unbalanced current-based tariff," *CIRED – Open Access Proc. Journal*, pp. 883-887, 2017.

Biographies

Aliasgar P. Shayer received his Bachelor of Engineering degree in electrical engineering from the Veer Narmad South Gujarat University, Surat, India, in 2010 and Master of Engineering degree from the Gujarat Technological University, Ahmedabad, India, in 2014 and is currently pursuing his Ph. D. degree from the Sardar Vallabhbhai National Institute of Technology, Surat, India. He is currently a research scholar in the Department of Electrical Engineering, Sardar Vallabhbhai National Institute of Technology. His research interests include the application of power electronics in power systems with a special focus of power flow management and power quality improvement of railway electrical power system.
E-mail: aliasgarshayer@gmail.com

Mahmadasraf A. Mulla received his Bachelor of Engineering degree in electrical engineering from the Sardar Vallabhbhai National Institute of Technology, Surat, India, in 1995 and Master of Engineering degree from the Maharaja Sayajirao University of Baroda, Vadodara, India, in 1997 and Ph.D. degree from Sardar Vallabhbhai National Institute of Technology, Surat, India, in January 2015. He is currently an Associate Professor in the Department of Electrical Engineering, at Sardar Vallabhbhai National Institute of Technology. His research interests include solar and wind energy conversion, electrical drives, power quality and active power filters.
E-mail: mamulla@ieee.org